# TITLE

Motion-Insensitive Determination of $B_1^+$ Amplitudes Based on the Bloch-Siegert Shift in Single Voxels of Moving Organs Including the Human Heart


## AUTHORS

Ayse Sila Dokumaci[1], Bertrand Pouymayou[1], Roland Kreis[1], and Chris Boesch[1]

## AUTHOR AFFILIATION

[1]Dept.Clinical Research and Dept.Radiology, University of Bern, Switzerland


## RUNNING TITLE

$B_1^+$ Amplitudes Based on Bloch-Siegert Shift in Moving Organs Including the Human Heart


## CORRESPONDING AUTHOR

Chris Boesch, PhD & MD

University Bern, AMSM (DKF/DIPR)

Pavilion 52A Inselspital, P.O. Box 35, CH-3010 Bern, Switzerland

e-mail: chris.boesch@insel.ch

phone: ++41-31-632-81-74


**WORD COUNT:** 4129 words of body text


## GRANT SPONSOR

Supported by the Swiss National Science Foundation #31003A-132935 and #310030-149779 to CB)

# ABSTRACT

**Purpose:** To reliably determine the amplitude of the transmit radiofrequency ($B_1^+$) field in moving organs like the liver and heart, where most current techniques are usually not feasible.

**Methods:** $B_1^+$ field measurement based on the Bloch-Siegert (BS) shift induced by a pair of Fermi pulses in a double-triggered modified Point RESolved Spectroscopy (PRESS) sequence with motion-compensated crusher gradients has been developed. Performance of the sequence was tested in moving phantoms and in muscle, liver, and heart of 6 healthy volunteers each, using different arrangements of transmit/receive coils.

**Results:** $B_1^+$ determination in a moving phantom was almost independent of type and amplitude of the motion and agreed well with theory. In vivo, repeated measurements led to very small coefficients of variance if the amplitude of the Fermi pulse was chosen above an appropriate level (CV in muscle 0.6 %, liver 1.6 %, heart 2.3 % with moderate amplitude of the Fermi pulses and 1.2 % with stronger Fermi pulses).

**Conclusion:** The proposed sequence shows a very robust determination of $B_1^+$ in a single voxel even under challenging conditions (transmission with a surface coil or measurements in the heart without breath-hold).



# KEYWORDS

$B_1^+$ determination

Radiofrequency fields

Bloch-Siegert shift

Moving organs

Single voxel

PRESS

# INTRODUCTION

In MRI and MRS, determining the amplitude of the $B_1^+$ field is crucial to adjust the transmitter gain which leads to the desired rotation of the magnetization by the applied radiofrequency (RF) pulses. While the adjustment of the mostly homogeneous RF field of a body coil is standard in commercially available scanners, the problem of $B_1^+$ field determination produced by surface coils and particularly in moving organs is far from being solved. Generally speaking, magnetic resonance based $B_1$ mapping methods can be divided into two groups as magnitude-based and phase-based methods (1,2).

The so-called Double Angle Methods (DAM) use the ratio of two images obtained with two different flip angles to calculate the $B_1^+$ field (3). In order to avoid the $T_1$ dependence, it is essential to use long repetition times (TR), which results in increased acquisition times. For that reason, time-efficient versions of DAM have been developed which include sequences that reset magnetization at the end of each acquisition, known as Saturated Double Angle Method (SDAM), or sequences that are combinations of DAM with fast imaging methods (4-6). Actual Flip Angle Imaging uses two identical RF pulses that are followed by different delays. While the method is quite insensitive to $T_1$ (7) and results in accurate $B_1^+$ field determinations, this method has some disadvantages which include sensitivity to flow, low signal-to-noise ratios (SNR) due to quick excitations, and possible inaccurate results because of insufficient spoiling of transverse magnetization (7-9). To overcome some of these limitations, derivatives of the method have been developed which include methods with better gradient and RF spoiling schemes (9) and methods that do not use the short TR approximation (8,10). Besides these, there are methods based on multi-pulse sequences like the three-pulse sequence which uses the ratio of stimulated echo and spin echo images (11). Along with other methods (12-18), magnitude-based methods comprise a larger part of $B_1$ mapping methods.

Phase-based methods cover those employing a pair of composite RF pulses (19), those using non-selective $180°_x$ and $90°_y$ pulses which act as $2\alpha$ and $\alpha$ pulses (20), and those which take advantage of adiabatic pulses (21-23). Their disadvantages include sensitivity to main field ($B_0$) inhomogeneities (7), requirement for long repetition times, the need for a $B_0$ map for off-resonance effects (20), and limitations due to specific absorption rate (SAR), respectively. A robust phase-based method for $B_1$ mapping uses the Bloch-Siegert (BS) shift phenomenon, which is the shift in the resonance frequency of nuclei when an off-resonance RF pulse is applied following excitation (1,24). This method was shown to be insensitive to TR, $T_1$

relaxation effects, chemical shift, $B_0$ inhomogeneities, and magnetization transfer (1,2). For spectroscopy applications, voxel-based $B_1^+$ field calculations based on a PRESS sequence can be designed such that they receive data exactly from the same volume as the subsequent signal acquisition (25).

Most of the methods are not feasible for moving organs and to the best of our knowledge, the only successful attempts of $B_1^+$ mapping in the heart were performed using a magnitude-based SDAM with spiral readouts (5,26,27), providing whole heart coverage. The examinations were performed in breath-hold during 16-20 heartbeats resulting in acquisitions as long as 25 s, which makes the method inherently susceptible to irregular heartbeats and poses additional problems in patients who have difficulties to hold their breath (5).

In this work, we aimed to develop and test a method that would provide a single-voxel $B_1^+$ amplitude measurement in the heart within a single heartbeat, such that the method could be combined with navigator triggering for the free breathing patient and ECG triggering for the heart. BS shift-based $B_1^+$ sensitization introduced in a PRESS sequence with motion-compensated crusher gradients offered the best approach to generate such a sequence. Even if an additional acquisition without BS effect is necessary to measure the reference phase, the two required heartbeats can be separated by an arbitrary time period and double-triggering without breath-hold is possible. Since some spectroscopy applications require the use of a transmit surface coil, we wanted to test the suggested sequence with different coil arrangements, including body, head, or surface coil transmission combined with either head or surface coil reception. The determination of $B_1^+$ amplitude during surface coil transmission is particularly important and also demanding since the field falls off rapidly with increasing distance from the coil. An additional challenge was the fact that no "gold standard" for the $B_1^+$ determination in the heart is available, which could be used for a comparison with the newly developed sequence. Therefore, the study was designed such that the methodological complexity was gradually increased (no motion to various types of motion; homogeneous transmission with a volume coil to surface coil excitation; experiments in a well defined phantom to measurements in muscle, liver, and finally heart in vivo).

# METHODS

Figure 1 illustrates the modified Point RESolved Spectroscopy (PRESS) sequence with motion-compensated crusher gradients (28,29) and two 8-ms-long Fermi pulses. This PRESS sequence can be double-triggered (navigator-triggered prospective acquisition correction [PACE] and ECG-triggering) and has been implemented on a 3T MR-system (VERIO, SIEMENS, Erlangen, Germany). Fermi pulses were symmetrically applied around the water resonance frequency, selectable at various offset frequencies including ± 2 kHz, ± 4 kHz, and ± 8 kHz. According to the notation of reference (1), the Bloch-Siegert shift $\Phi_{BS}$ ,i.e. the phase difference between two scans with and without Fermi pulse can be calculated as:

$$\phi_{BS} = (B_{1,peak})^2 * \mathrm{K_{BS}} \quad [1]$$

$$\mathrm{K_{BS}} = \int_0^T \frac{(\gamma B_{1,normalized}(t))^2}{2\omega_{RF}(t)} dt \quad [2]$$

where T is the pulse duration and γ the gyromagnetic ratio. $K_{BS}$ is a pulse specific parameter which is proportional to the area under the (normalized) pulse envelope and inversely proportional to the off-resonance frequency ($\omega_{RF}$) for the Fermi pulses (1). Both Fermi pulses were programmed to match their $K_{BS}$ value to 74.01 [rad/G$^2$] for the ± 4 kHz offset case, which was the value used in the original BS shift-based $B_1^+$ mapping method (1). For a pulse with constant offset frequency as used here, $\omega_{RF}$ can be extracted from $K_{BS}$, leading to:

$$\phi_{BS} = (B_{1,peak})^2 * \frac{1}{\omega_{RF}} * \mathrm{k}_{Fermi} \quad [3]$$

$$\mathrm{k}_{Fermi} = \int_0^T \frac{(\gamma B_{1,normalized}(t))^2}{2} dt \quad [4]$$

$$\mathrm{B}_{1,peak} = \sqrt{\frac{\phi_{BS} * \omega_{RF}}{\mathrm{k}_{Fermi}}} \quad [5]$$

with $k_{Fermi}$ = 29.60 [rad*Hz/μT$^2$]. In the current implementation, the Fermi pulses are applied twice such that $k_{2*Fermi}$ = 59.20 [rad*Hz/μT$^2$].

Crusher gradients with two lobes in the standard PRESS sequence were converted into motion-compensated crusher gradients having four lobes such that the net zeroth, first, and second moments would be equal to zero. For each two-lobe-part, the net area obviously needs to be non-zero to act as a crusher for unwanted excitations. The latter two-lobe-part was

implemented so that it would be applied after the Fermi pulse to remove also the unwanted signals that could be caused by the Fermi pulse.

Following validation by in vitro experiments using a spherical phantom at rest and with motion, the sequence was applied on skeletal muscle and liver in one group of 6 healthy volunteers (3 males, 3 females, age 24.7 ± 2.5y, BMI 23.2 ± 3.0 kg/m$^2$) and in the heart of another group of 6 healthy subjects (5 males, 1 female, age 30.2 ± 3.8y, BMI 24.4 ± 1.8 kg/m$^2$). Informed consent was obtained from all volunteers and the study was approved by the Institutional Ethical Committee. Different types of coils were used to evaluate possible coil specific problems. In vitro experiments were performed using a transmit/receive (Tx/Rx) volume coil ($^1$H/$^{31}$P head coil, RAPID Biomedical, Rimpar, Germany) and a Tx/Rx surface coil ($^1$H/$^{31}$P, RAPID Biomedical, Rimpar, Germany). While skeletal muscle and liver were measured with the same surface coil used for the phantom experiments, body coil transmission was combined with reception using spine matrix coil and body array coil for the heart measurements.

A phantom (diameter 17 cm, "braino phantom", General Electric, Milwaukee) was measured at rest and during various types of motion with different speeds and amplitudes generated by a home-built device located inside the scanner room. The displacement in the positive direction was controlled by a servo-motor while the phantom was pulled back to its initial position by a spring force. Two different speeds and amplitudes were used to test motion dependence and were adjusted to resemble the breathing motion determined by a navigator sequence as much as possible. Single-shot measurements were taken from a voxel size of 20x20x20mm with an echo time of 64.2 ms and a repetition time of 1500 ms. Fermi pulses were applied at offset frequencies of ± 2 kHz, ± 4 kHz, and ± 8 kHz with varying voltages in order to validate the expected behavior of the BS shift-based phase change in the phantom using a volume coil. Surface coil measurements were performed in the phantom by applying the pulses only at ± 2 kHz offset frequencies as in the in vivo measurements.

Measurement parameters for the resting skeletal muscle (m.quadriceps femoris) included a voxel size of 20x20x20mm, an echo time of 64.2 ms, and a repetition time of 1500 ms like the phantom examinations. The sequence was applied with PACE-triggering in liver due to respiratory motion and also in breath-hold for comparison. Voxel sizes in the liver varied between 20x30x25mm and 40x40x40mm. Echo time used for the liver was 64.2 ms while the repetition time was either 1500 ms in breath-hold or determined by the trigger signal. Measurements in the heart were taken in PACE/ECG double triggering mode as described in

Ith et al. (30) to freeze respiratory and cardiac motion with a voxel size of 12x25x20mm positioned in the cardiac septum and a repetition time defined by the respiration rate. ECG trigger delay (typically 250 ms) was adjusted such that the sequence started in the late contraction/beginning relaxation phase. In order to test the variation of the measured BS shift, 16 repetitions of single-shot measurements were acquired in the heart with a scan time of approximately 2 minutes.

Except for the heart, DICOM files of single coil receptions were analyzed using MATLAB (The MathWorks, Inc.). Due to the array coil arrangement used in the heart and thus inherent phase adjustment between the single coils in the DICOM file, which made a determination of the BS shift impossible, raw data from the scanner had to be analyzed using a modified version of the MATLAB program provided by Maolin Qiu at Yale University (SIEMENS IDEA forum). The $B_1^+$ amplitude was calculated from the phase difference of two single-shot acquisitions with and without the application of Fermi pulses according to the relation given in Eq. [1]. The phase was calculated from the first point in the time domain signal for each scan, since the first point corresponds to the echo top and contains most of the signal information.

$B_1^+$ maps from a work-in-progress $B_1^+$ mapping package (3P-MAP, based on the stimulated vs. spin echo responses for a 3-pulse sequence, duration 17 s, SIEMENS, Erlangen, Germany) were obtained for comparison in all cases except for the heart where the $B_1^+$ determination was not feasible because the 3P-MAP sequence did not have PACE/ECG double triggering options. The scanner provides a reference voltage (REF) that corresponds to a 90 degree excitation by a rectangular 500 μs pulse, i.e., to a $B_1^+$ field of 11.75 μT. The determination of REF is reliable as long as homogeneous excitation fields (e.g. body coil) are used; however, with surface coil excitation, it often underestimates the required RF power since the algorithm uses the high intensity signal from the regions close to the coil.

To describe the repeatability, coefficients of variance were calculated. Agreement between the two $B_1^+$ methods was calculated based on the Lin's Concordance Correlation Coefficient (MATLAB, The MathWorks, Inc.).

# RESULTS

In order to compare the behavior of the BS shift effect in the phantom with theory, Fermi pulses were applied using four different voltages (120, 180, 240, 300 V with the transmitter reference voltage being 174 V) and three different frequency offsets. Fig.2 shows these stationary and moving phantom results for the induced phase change with respect to the reference scan. Black curves, representing the fitted data for the non-moving phantom, are almost perfectly aligned with the measured values of the non-moving phantom. The single BS shift-based $B_1^+$ measurements of the non-moving phantom (red crosses, 15 single-shot repetitions) are indistinguishable. When the motion was started with very fast speed and large amplitude, the measured phase changes became slightly (average CV of 4.9%) scattered (blue crosses) without systematic under- or overestimation of the theoretical curve for the non-moving phantom. BS shift-based $B_1^+$ measurements determined the $B_1^+$ amplitude as 0.065 μT/V (SD 0.001 μT/V) for the stationary case (black curve) and 0.067 μT/V (SD 0.002 μT/V, curve not shown) for the moving case. 3P-MAP was repeated three times for the stationary case giving a $B_1^+$ amplitude of 0.066 μT/V (SD 0.002 μT/V) in the voxel in all repetitions. The scanner adjustment corresponds to the $B_1^+$ amplitude as 0.068 μT/V; however, determined over the whole 17 cm-diameter phantom.

A comparison between the BS shift-based $B_1^+$ measurement and the 3P-MAP in the phantom using the double-tuned surface coil for different types of motion is displayed in Fig.3. Average values and error bars, representing the standard deviations, are shown for 10 single-shot measurements for the BS shift-based $B_1^+$ measurement and 10 repetitions of the 17-second-long 3P-MAP sequence. It is evident that with increasing speeds and amplitudes, the standard deviation of the 3P-MAP increased. In addition, a systematic overestimation of the $B_1^+$ field was observed even with slow motion. In contrast, the BS shift-based $B_1^+$ measurement continued to produce consistent results. For the fast motion with large amplitude, standard deviation of the 10 single-shot measurements for the BS shift-based $B_1^+$ measurement for the calculated flip angle was 0.0384 radians.

The resting muscle was used to compare the 3P-MAP with the newly developed BS shift-based sequence in an organ without motion but with a very inhomogeneous $B_1^+$ profile of the transmitting surface coil (explaining the large differences between subjects). Figure 4 shows the comparison between the single-shot measurements of the BS shift-based $B_1^+$ measurement and the repetitions of the 3P-MAP sequence. Lin's Concordance Correlation Coefficient was

calculated as 0.98 for the two methods with a calculated mean flip angle difference of 0.0227 radians. A test of repeatability of the BS shift-based sequence in 15 single-shot repetitions each in 6 volunteers resulted in an average coefficient of variation (CV) of 0.6%.

The next in vivo tests were performed in the liver in order to compare 3P-MAP with BS shift-based $B_1^+$ measurements in a slowly moving organ. Since motion during the application of the gradients leads to phase shifts, BS shift-based $B_1^+$ measurements were applied both in breath-hold and with triggering to test the efficiency of the motion-compensation. Figure 5 demonstrates the results for the triggered BS shift-based $B_1^+$ measurement (16 single-shot measurements), the breath-hold BS shift-based $B_1^+$ measurement (7 single-shot measurements), and the 3P-MAP sequence (3 repetitions of breath-hold measurements). Lin's Concordance Correlation Coefficient for the triggered BS and breath-hold BS measurements was 0.92 and the mean $B_1^+$ amplitude difference was 0.069 μT (SD 0.090 μT). While the two BS-based methods agree very well (Bland-Altman plot Fig.5B), the 3P-MAP shows significantly higher $B_1^+$ amplitudes than those measured by the BS shift-based method (Bland-Altman plots in Fig.5C and 5D). The same behavior has been observed in the moving phantom where the BS-based method was not influenced by the motion (Fig.3). Mean $B_1^+$ amplitude difference between the triggered BS shift-based measurements and 3P-MAP measurements was 1.33 μT (SD 0.14 μT). A test of repeatability of the triggered BS shift-based sequence using surface coil transmission was performed in the liver of 6 volunteers in 16 single-shot repetitions each and resulted in an average CV of 1.6%.

The heart with two independent motions of the respiratory and cardiac action represents the most challenging organ for motion-sensitive sequences. Figure 7 illustrates the changes in the repetitions of the single-shot measurements when the Fermi pulses were applied at different voltages relative to the transmitter reference voltage for all volunteers. Similar to the muscle and liver results, single-shot repetitions were stable with an average CV of 2.3 % for the $B_1^+$ amplitude change due to the BS shift for 16 single-shot repetitions in 6 volunteers when the Fermi pulses were applied at the transmitter reference voltage. Above the reference voltage, the variations were even lower (1.2 %, measured in 5 subjects only) while the results were not optimal when the Fermi pulse voltages were below the REF voltage (CV of 7.5 %). $B_1^+$ amplitudes (generated by the body coil) were calculated as 10.52 μT, 9.33 μT, 10.43 μT, 10.07 μT, 13.55 μT, and 9.85 μT in different subjects. The relative difference between the subject with the strongest and weakest $B_1^+$ in the ventricular septum (9.33 μT for a male 1.93 m tall and weight of 100 kg, vs. 13.55 μT for a female 1.57 m tall and weight of 57 kg) is

37% (difference/average) and would correspond to excitation angles of 62 degrees vs. 90 degrees if the RF field would not be adjusted to the value in the voxel.

# DISCUSSION AND CONCLUSIONS

The suggested PACE/ECG-triggered PRESS sequence reveals reliable measurements of $B_1^+$ with single-shot acquisitions (applied twice - once with BS shift and once without). It is almost immune against motion related perturbations and can also be applied in the heart. The sequence has been validated in vitro and in vivo in various organs and with different coil arrangements.

To begin with, the fitted curves of the measurements in the phantom confirm the theoretically expected behavior with the quadratic phase increase with the Fermi voltage as well as the linear phase increase with the offset frequency (see Fig.4). Measurements during motion are almost identical to the measurements without motion and the variations are still very small, proving the robustness of the sequence against motion in vitro. In addition to the compliance with theory, the results agree well with the 3P-MAP results when the 3P-MAP is applied in the phantom at rest.

The variation among the repetitions of the single-shot measurements in motionless organs like the quadriceps muscle is very small when the BS shift-based sequence is applied. Comparison of the sequences in the muscle and the high concordance correlation coefficient indicate the high level of agreement between the two methods in an immobile organ where the 3P-MAP can be used as a "gold-standard" for the newly developed sequence. Since only the 3P-MAP deteriorates with motion while the BS-based $B_1^+$ values remain stable, we conclude that the values measured by the BS-shift method are accurate, even if there is no longer a "gold-standard" to compare with.

Single-shot measurements in the heart are highly reproducible with small variances as long as the nominal Fermi voltage is above a threshold value like the transmitter reference voltage determined by the scanner. Lower Fermi pulse voltages resulted in larger noise of the phase shift and thus of the $B_1^+$ value. This observation is important since the specific absorption rate (SAR) of the Fermi pulse is relatively high and imaging implementations of the BS technique tend to choose smaller Fermi pulse amplitudes; however, for MR spectroscopy sequences with long TR and few acquisitions, this does not apply. Since 3P-MAP does not work in heart due to the lack of double-triggering, agreement between BS shift-based sequence and 3P-MAP cannot be shown.

The original BS shift-based $B_1^+$ mapping sequences, which were modifications of spin echo and gradient echo sequences, were applied in the abdomen as a moving organ without breath-hold (1). Since the sequence was not motion-compensated, artifacts in the phase-encoding direction were reported even though they were stated not to affect the results significantly (1). In the heart, due to motion complexity, this method would be insufficient without motion-compensated gradients. Besides the successful tests for $B_1^+$ mapping in the heart using a magnitude-based SDAM with spiral readouts (5,26,27), we were able to determine the single-voxel $B_1^+$ amplitude in the heart for the first time using a phase-based $B_1^+$ measurement method without the need of a breath-hold. It will be highly beneficial to single-voxel MRS measurements in the heart or in any organ especially when surface coils are used since the adjustment routine from the scanner seemed to be insufficient for the flip angle calibration. The 37% $B_1^+$ value difference between two subjects illustrates the importance of a localized determination of the RF field strength in the heart. Without adjusting the RF power for the heart, the flip-angles for the two subjects would differ as 90 degrees to 62 degrees resulting in a considerable reduction of signal quality, e.g. in a PRESS selected spectrum. Based on an earlier study on heart lipids without a localized determination of $B_1^+$ (30), we assume that insufficient RF adjustment is responsible for a considerable fraction of low quality spectra. The direct consequences of incorrect $B_1^+$ adjustment for spectral quality and accuracy have not been shown experimentally in this study; however, there are many publications which show the crucial influence of this adjustment e.g. on the pulse profile and thus for the shape of the voxel (25,27), signal contamination from neighboring tissues, and also for overall signal magnitude.

Phase dependent methods have to solve the problem of phase wrapping, in particular in imaging mode where large differences of regional $B_1^+$ may occur. In the proposed single voxel sequence, even if phase wrapping occurred between the acquisitions with vs. without Fermi pulse, unwrapping was straightforward if the Fermi pulse strength was chosen appropriately, i.e. approximately at the REF level such that the effect was large enough to generate sufficient effects, yet small enough to be below 2*PI.

An inherent strength of the Bloch-Siegert effect is its independence of the signal amplitude which makes it particularly suited for triggered acquisitions where the TR can change depending on the breathing and/or cardiac cycle. Under these conditions, amplitude-based methods need special corrections; however, Bloch-Siegert shift based methods are immune against variations in amplitude and hence TR.

Another strength of phase-based methods is the fact that the first point in the FID (or central part of the echo) contains the full phase information; i.e. the sequence is inherently short which is beneficial in moving organs since it is not necessary to acquire the full acquisition window.

The major limitation of the current method is its single-voxel nature, giving accurate values for a specific location, yet not for the complete volume. For single-voxel MR spectroscopy, this limitation is not a problem; however, if data acquisition on a whole volume is required, for instance to correct for absolute quantities of a CSI experiment or a FID acquisition, this limitation would be severe. 2D-Spiral readout methods could be combined with the sequence; however, at the price of a longer acquisition window.

Because it was aimed as a proof of principle, we did not try to shorten the sequence duration for the experiments further. Nevertheless, removing the second Fermi pulse from the sequence and instead of the reference scan without the BS shift, applying the only Fermi pulse with the negative frequency offset is a first step towards shortening the sequence. Fermi pulses were applied with positive and negative offsets in the same scan in order to avoid problems that might occur between different scans. Combining the crusher lobes with the refocusing lobe of the slice-selection gradient and combining all crusher gradients with fewer lobes after recalculating the moments further shorten the sequence. By performing these modifications, it was already possible to reduce the echo time from 64.2 ms to 42.6 ms. An additional potential for a shorter sequence is reducing the duration of the Fermi pulses which are relatively long.

Another limitation of the sequence is the fact that the slice selection gradients and the refocusing gradients were only balanced for zeroth moments. However, these gradients were considerably smaller than the crusher gradients and their possible effects on the phase due to motion would be minimal.

Using surface coils for transmission poses specific problems due to the large range of $B_1^+$ strengths and the possibility of hotspots close to the coil. Nonetheless, some spectroscopy applications (in particular the combination with non-proton nuclei) require surface coils where also the proton-part is integrated (e.g. for decoupling). The determination of $B_1^+$ is particularly crucial for such an arrangement; however, a single voxel sequence can only provide the field strength in one part of the tissue.

SAR issues due to the long Fermi pulses should not be a major problem thanks to the small number of only 2 scans in a final implementation and since the acquisition and the reference scan can be separated by an arbitrarily long period. The much larger number of scans in the current study served only to test the repeatability and will not be necessary in a final implementation where two scans are sufficient.

In conclusion, results suggest that the new BS shift-based PACE/ECG-triggered modified PRESS sequence is a robust and fast method for $B_1^+$ amplitude determination in a single voxel within moving organs.

# ACKNOWLEDGEMENTS

The authors thank SIEMENS (Erlangen, Germany) for providing the work-in-progress packages for $B_1^+$ mapping and navigator-triggered prospective acquisition correction (PACE); and Karin Zwygart for organizing volunteers and data storage.

# REFERENCES


1. Sacolick LI, Wiesinger F, Hancu I, Vogel MW. B1 mapping by Bloch-Siegert shift. Magn Reson Med 2010;63:1315-1322.

2. Sacolick LI, Sun L, Vogel MW, Dixon WT, Hancu I. Fast radiofrequency flip angle calibration by Bloch-Siegert shift. Magn Reson Med 2011;66:1333-1338.

3. Insko EK, Bolinger L. Mapping of the radiofrequency field. J Magn Reson Series A 1993;103:82-85.

4. Stollberger R, Wach P. Imaging of the active B1 field in vivo. Magn Reson Med 1996;35:246-251.

5. Cunningham CH, Pauly JM, Nayak KS. Saturated double-angle method for rapid B1+ mapping. Magn Reson Med 2006;55:1326-1333.

6. Wang D, Zuehlsdorff S, Larson AC. Rapid 3D radiofrequency field mapping using catalyzed double-angle method. NMR Biomed 2009;22:882-890.

7. Yarnykh VL. Actual flip-angle imaging in the pulsed steady state: a method for rapid three-dimensional mapping of the transmitted radiofrequency field. Magn Reson Med 2007;57:192-200.

8. Fleysher R, Fleysher L, Inglese M, Sodickson D. TROMBONE: T1-relaxation-oblivious mapping of transmit radio-frequency field (B1) for MRI at high magnetic fields. Magn Reson Med 2011;66:483-491.

9. Nehrke K. On the steady-state properties of actual flip angle imaging (AFI). Magn Reson Med 2009;61:84-92.

10. Hurley SA, Yarnykh VL, Johnson KM, Field AS, Alexander AL, Samsonov AA. Simultaneous variable flip angle-actual flip angle imaging method for improved accuracy and precision of three-dimensional T1 and B1 measurements. Magn Reson Med 2012;68:54-64.

11. Akoka S, Franconi F, Seguin F, Le PA. Radiofrequency map of an NMR coil by imaging. Magn Reson Imaging 1993;11:437-441.

12. Nehrke K, Bornert P. DREAM--a novel approach for robust, ultrafast, multislice B(1) mapping. Magn Reson Med 2012;68:1517-1526.

13. Dowell NG, Tofts PS. Fast, accurate, and precise mapping of the RF field in vivo using the 180 degrees signal null. Magn Reson Med 2007;58:622-630.

14. Murphy-Boesch J, So GJ, James TL. Precision mapping of the B1 field using the rotating-frame experiment. J Magn Reson 1987;73:293-303.

15. Hornak JP, Szumowski J, Bryant RG. Magnetic field mapping. Magn Reson Med 1988;6:158-163.

16. Klose U. Mapping of the radio frequency magnetic field with a MR snapshot FLASH technique. Med Phys 1992;19:1099-1104.

17. Chung S, Kim D, Breton E, Axel L. Rapid B1+ mapping using a preconditioning RF pulse with TurboFLASH readout. Magn Reson Med 2010;64:439-446.

18. Eggenschwiler F, Kober T, Magill AW, Gruetter R, Marques JP. SA2RAGE: a new sequence for fast B1+ -mapping. Magn Reson Med 2012;67:1609-1619.

19. Oh CH, Hilal SK, Cho ZH, Mun IK. Radio frequency field intensity mapping using a composite spin-echo sequence. Magn Reson Imaging 1990;8:21-25.

20. Morrell GR. A phase-sensitive method of flip angle mapping. Magn Reson Med 2008;60:889-894.

21. Park, J. Y. and Garwood, M. B1 Mapping Using Phase Information Created by Frequency-Modulated Pulses. Proceedings of the 16th Annual Meeting of ISMRM Toronto, Ontario, Canada 2008. Abstract 361.

22. Hennel, F. and Köhler, S. Improved Phase-Based Adiabatic B1 Mapping. Proceedings of the 18th Annual Meeting of ISMRM Stockholm, Sweden 2010. Abstract237.

23. Jordanova KV, Nishimura DG, Kerr AB. B estimation using adiabatic refocusing: BEAR. Magn Reson Med 2014;72:1302-1310.

24. Bloch F, Siegert A. Magnetic resonance for nonrotating fields. Phys Rev 1940;57:522-527.

25. Noeske, R., Schulte, R., and Schirmer, T. Voxel Based Transmit Gain Calibration using Bloch-Siegert Shift Method for MR Spectroscopy. Proceedings of the 20th Annual Meeting of ISMRM Melbourne, Australia 2012. Abstract 1733.

26. Sung K, Nayak KS. Measurement and characterization of RF nonuniformity over the heart at 3T using body coil transmission. J Magn Reson Imaging 2008;27:643-648.

27. Schar M, Vonken EJ, Stuber M. Simultaneous B(0)- and B(1)+-map acquisition for fast localized shim, frequency, and RF power determination in the heart at 3 T. Magn Reson Med 2010;63:419-426.

28. Bernstein MA, King Kevin F., Zhou Xiaohong Joe. Gradient Moment Nulling. Handbook of MRI Pulse Sequences. Burlington, MA: Elsevier Academic Press; 2004. p 331-49.

29. Duan Q, van GP, Duyn J. Improved Bloch-Siegert based B1 mapping by reducing off-resonance shift. NMR Biomed 2013;26:1070-1078.

30. Ith M, Stettler C, Xu J, Boesch C, Kreis R. Cardiac lipid levels show diurnal changes and long-term variations in healthy human subjects. NMR Biomed 2014;27:1285-1292.

# FIGURE CAPTIONS

Figure 1:

Diagram of the proposed sequence with motion-compensated crusher gradients (cyan) and 8 ms long Fermi pulses (yellow) following the 180°-pulses (red). Fermi pulses are applied at symmetric offset frequencies (+ and -) with respect to the water resonance frequency. The sequence can be preceded by a navigator-triggered prospective acquisition correction trigger (PACE, not shown) and can also be ECG-triggered.

Figure 2:

Phase changes as a function of Fermi pulse voltage and frequency offset for a phantom without motion (blue crosses, indistinguishable for the 15 repetitions each) and with motion (red crosses showing 15 repetitions each) in a volume transmit/receive coil. The black line represents the fit of the measurements without motion with the theoretical behavior according to Eq. [3] (scaling of the curve with 0.1245 Hz*rad/V$^2$), resulting in a $B_1^+$ amplitude of 0.0648 µT/V. The fit of the measurements with motion resulted in a $B_1^+$ amplitude of 0.0673 µT/V. As a comparison, the 3P-MAP method repeated three times for the stationary case gave a $B_1^+$ amplitude of 0.0660 µT/V for the selected voxel, while the scanner adjustment for the whole object determined a value of 0.0675 µT/V.

Figure 3:

Influence of motion (speed and amplitude) on the $B_1^+$ field determination by the BS shift-based $B_1^+$ acquisition (blue) and 3P-MAP sequence (red), using surface coil transmission and reception in vitro (10 repetitions each). Without motion, the two methods agree very well while increasing motion (in amplitude and speed) deteriorates the results of the 3P-MAP sequence resulting in large variations and systematically overestimated values. The BS shift-based acquisition shows only a small increase of the variation between the 10 repetitions without a systematic bias. Error bars represent the standard deviation.

Figure 4:

Comparison of $B_1^+$ field amplitudes determined by the BS shift-based $B_1^+$ sequence and 3P-MAP in human quadriceps muscle. Different locations for the voxels in the inhomogeneous $B_1^+$ field of a surface coil transmission mainly explain the variations between subjects. In addition, different coil loading could add to the variations since a fixed transmitter voltage was used for all subjects.

Figure 5

5A) Comparison of the $B_1^+$ measurements in liver with 3P-MAP (black crosses, 3 repetitions), triggered BS shift-based measurements (red crosses, 16 repetitions) and BS shift-based results in breath-hold (blue crosses, 7 repetitions) for 6 subjects. Differences between the subjects are mainly a consequence of the voxel position. A comparison of the three methods is shown by Bland-Altman plots (identical vertical scale) between (B) triggered BS shift-based measurements vs. BS shift-based results in breath-hold, (C) triggered BS shift-based

measurements vs. 3P-MAP; and (D) BS shift-based results in breath-hold vs. 3P-MAP. In order to obtain the same number of examinations for both methods as required in the Bland-Altman plots, only the first 7 repetitions shown in (A) were used in (B) and 3 in (C) and (D), respectively. The comparison of the two BS-based examinations in (B) shows very good agreement (zero included in the error range which is small) while the comparisons of BS-based results with 3P-MAP in (C) and (D) show a significant difference (zero outside the error range of 1.96 standard deviations).

Figure 6

Radiofrequency field strength ($B_1^+$) for the 16 repetitions (each with vs. without Fermi pulses) in the heart of 6 volunteers (body coil transmission, surface coil detection) with various amplitudes of the Fermi pulse (relative to "REF" = voltage which is determined by the vendor's adjustment routine). The curves in grey were acquired with Fermi pulses below the REF voltage and show relatively large variations while the curves in red and blue were measured at the REF voltage and above, respectively, and show very high reproducibility within the 16 repetitions.

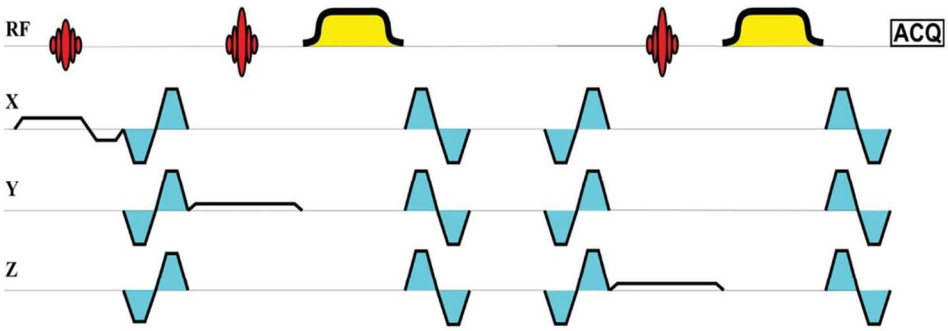


Figure 1:
Diagram of the proposed sequence with motion-compensated crusher gradients (cyan) and 8 ms long Fermi pulses (yellow) following the 180°-pulses (red). Fermi pulses are applied at symmetric offset frequencies (+ and -) with respect to the water resonance frequency. The sequence can be preceded by a navigator-triggered prospective acquisition correction trigger (PACE, not shown) and can also be ECG-triggered.
90x34mm (300 x 300 DPI)

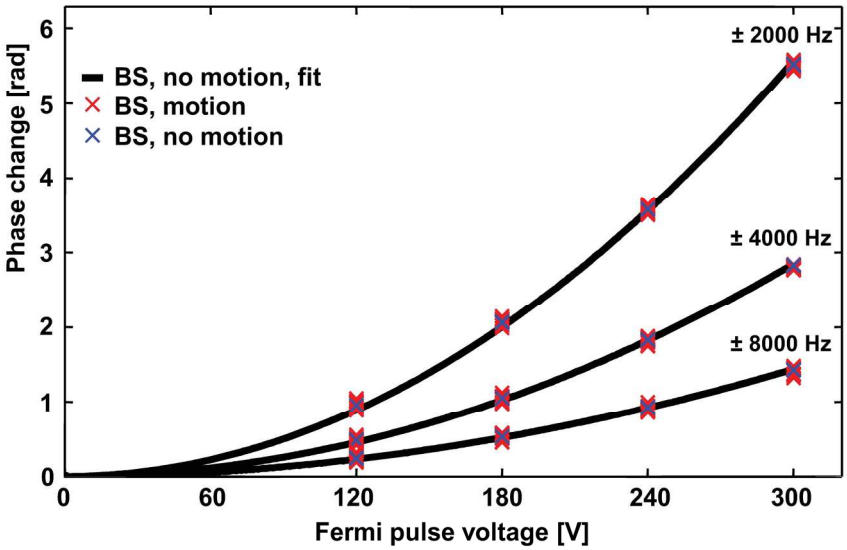


Figure 2:
Phase changes as a function of Fermi pulse voltage and frequency offset for a phantom without motion (blue crosses, indistinguishable for the 15 repetitions each) and with motion (red crosses showing 15 repetitions each) in a volume transmit/receive coil. The black line represents the fit of the measurements without motion with the theoretical behavior according to Eq. [3] (scaling of the curve with 0.1245 Hz*rad/V2), resulting in a sub>$1^{+}$ amplitude of 0.0648 µT/V. The fit of the measurements with motion resulted in a $B_1^{+}$ amplitude of 0.0673 µT/V. As a comparison, the 3P-MAP method repeated three times for the stationary case gave a $B_1^{+}$ amplitude of 0.0660 µT/V for the selected voxel, while the scanner adjustment for the whole object determined a value of 0.0675 µT/V.
190x142mm (300 x 300 DPI)

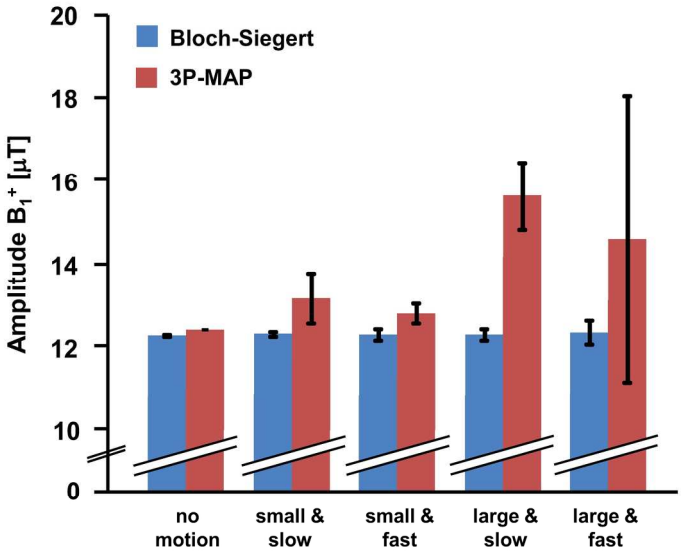


Figure 3:
Influence of motion (speed and amplitude) on the $B_1^+$ field determination by the BS shift-based $B_1^+$ acquisition (blue) and 3P-MAP sequence (red), using surface coil transmission and reception in vitro (10 repetitions each). Without motion, the two methods agree very well while increasing motion (in amplitude and speed) deteriorates the results of the 3P-MAP sequence resulting in large variations and systematically overestimated values. The BS shift-based acquisition shows only a small increase of the variation between the 10 repetitions without a systematic bias. Error bars represent the standard deviation.
190x142mm (300 x 300 DPI)

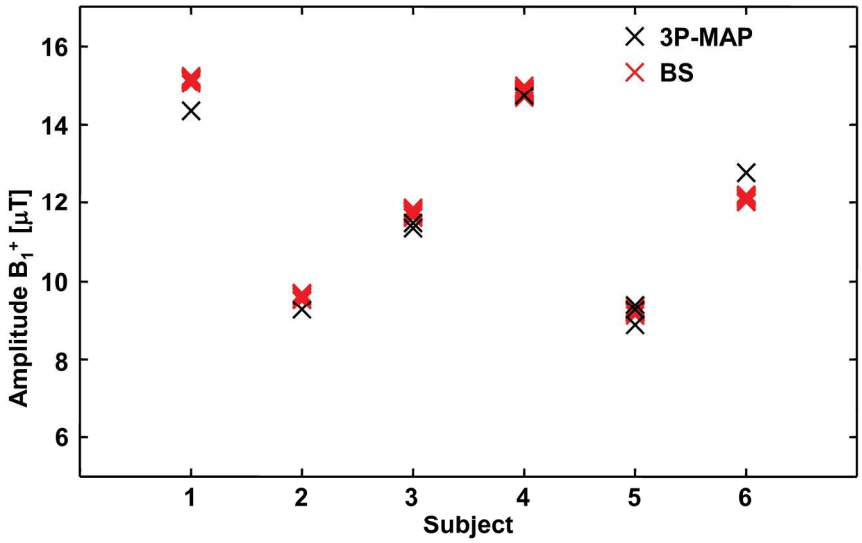


Figure 4:
Comparison of $B_1^+$ field amplitudes determined by the BS shift-based $B_1^+$ sequence and 3P-MAP in human quadriceps muscle. Different locations for the voxels in the inhomogeneous $B_1^+$ field of a surface coil transmission mainly explain the variations between subjects. In addition, different coil loading could add to the variations since a fixed transmitter voltage was used for all subjects.
190x142mm (300 x 300 DPI)

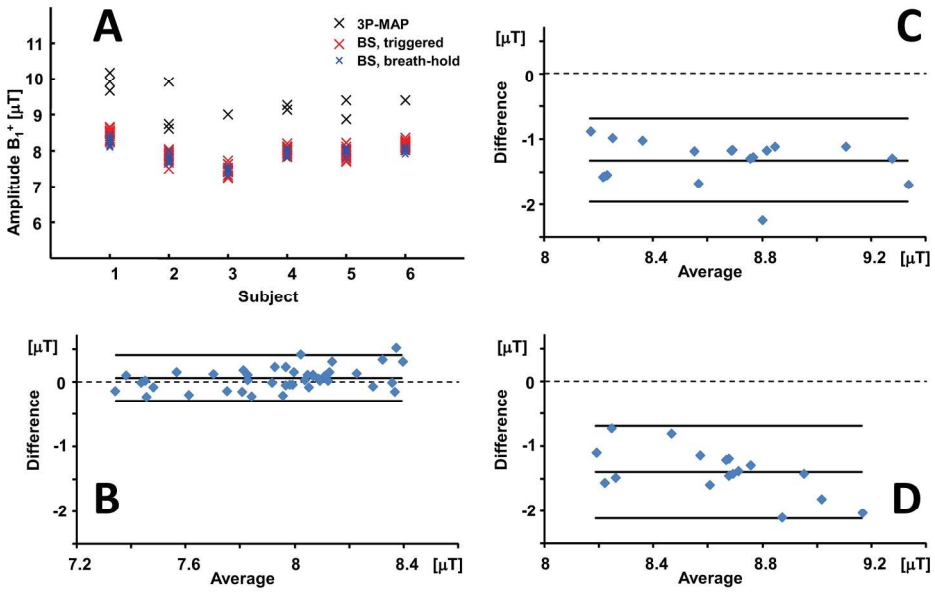


Figure 5:
5A) Comparison of the $B_1^+$ measurements in liver with 3P-MAP (black crosses, 3 repetitions), triggered BS shift-based measurements (red crosses, 16 repetitions) and BS shift-based results in breath-hold (blue crosses, 7 repetitions) for 6 subjects. Differences between the subjects are mainly a consequence of the voxel position. A comparison of the three methods is shown by Bland-Altman plots (identical vertical scale) between (B) triggered BS shift-based measurements vs. BS shift-based results in breath-hold, (C) triggered BS shift-based measurements vs. 3P-MAP; and (D) BS shift-based results in breath-hold vs. 3P-MAP. In order to obtain the same number of examinations for both methods as required in the Bland-Altman plots, only the first 7 repetitions shown in (A) were used in (B) and 3 in (C) and (D), respectively. The comparison of the two BS-based examinations in (B) shows very good agreement (zero included in the error range which is small) while the comparisons of BS-based results with 3P-MAP in (C) and (D) show a significant difference (zero outside the error range of 1.96 standard deviations).

190x142mm (300 x 300 DPI)

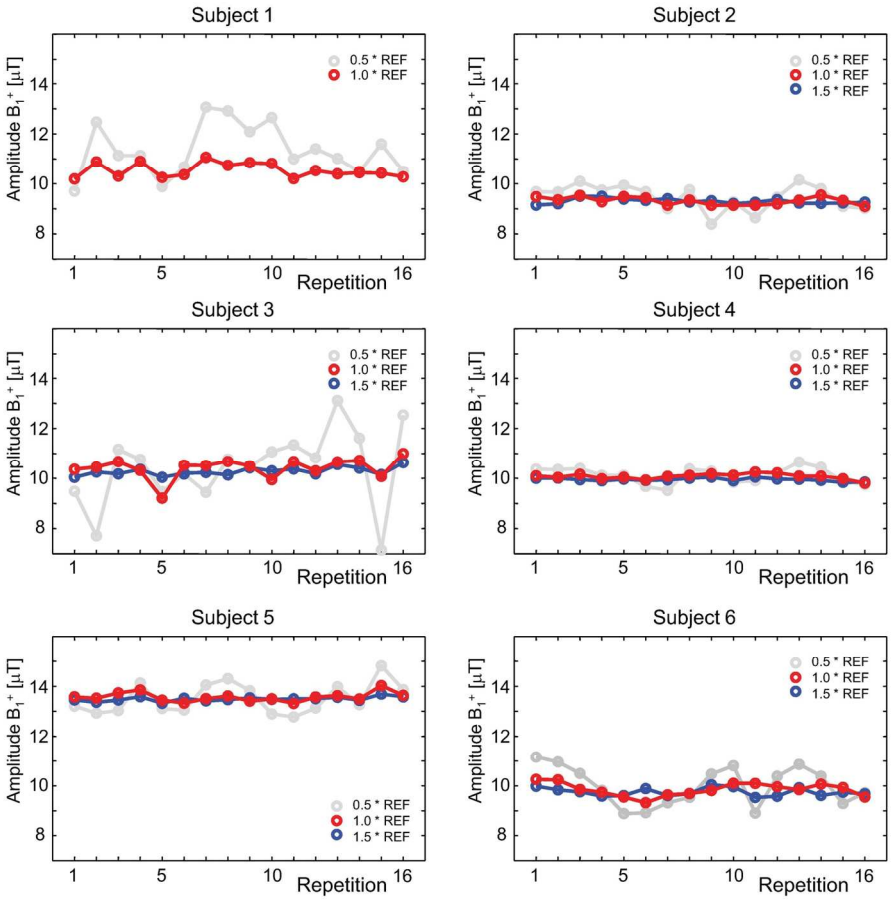


Figure 6:
Radiofrequency field strength ($B_1^+$) for the 16 repetitions (each with vs. without Fermi pulses) in the heart of 6 volunteers (body coil transmission, surface coil detection) with various amplitudes of the Fermi pulse (relative to "REF" = voltage which is determined by the vendor's adjustment routine). The curves in grey were acquired with Fermi pulses below the REF voltage and show relatively large variations while the curves in red and blue were measured at the REF voltage and above, respectively, and show very high reproducibility within the 16 repetitions.

155x151mm (300 x 300 DPI)